Asymmetric Little spin-glass model

R. Brunetti
Dipartimento di Fisica, Università di Napoli, "Federico II," Mostra D'Oltremare, Pad. 19, 80125 Napoli, Italy

G. Parisi
Dipartimento di Fisica, Università di Roma II, "Tor Vergata," Via Emanuele Carnevale, I-00173, Roma, Italy

F. Ritort
Dipartimento di Fisica, Università di Roma II, "Tor Vergata," Via Emanuele Carnevale, I-00173, Roma, Italy and Department de Física Fonamental, Universitat de Barcelona, Diagonal 648, 08020 Barcelona, Spain
(Received 5 August 1991; revised manuscript received 27 March 1992)

We study the static properties of the Little model with asymmetric couplings. We show that the thermodynamics of this model coincides with that of the Sherrington-Kirkpatrick model, and we compute the main finite-size corrections to the difference of the free energy between these two models and to some clarifying order parameters. Our results agree with numerical simulations. Numerical results are presented for the symmetric Little model, which show that the same conclusions are also valid in this case.

I. INTRODUCTION

Encouraged by some numerical results on the exact evaluation of the partition function for small systems,[1] which signaled the possibility of different behavior between the Little spin-glass model[2] and the Sherrington-Kirkpatrick (SK) model,[3] we have performed an extensive study of their static properties in order to see to what extent they differ.

The Little model consists of two sets of N spins $\{\sigma_i,\tau_i; i=1,\ldots,N\}$ and the interaction is governed by the Hamiltonian

$$H=-\sum_{i\neq j}J_{ij}\sigma_i\tau_j \ , \tag{1}$$

where J_{ij} are quenched variables with zero mean and variance $1/N$. When the coupling matrix is symmetric ($J_{ij}=J_{ji}$), we have the symmetric Little model. On the contrary, if J_{ij} and J_{ji} are uncorrelated variables, we have the asymmetric Little model.

The symmetric Little model, which has been applied in the context of neural networks,[4] gives the dynamics of a neural net with parallel updating. Cabasino *et al.*[1] have studied the eigenstates and limit cycles of the SK model, performing a parallel updating of the spins. In their numerical results, done at $T=0$, it was shown that the energy of the lowest-lying limit cycles was clearly lower than that obtained for the lowest eigenstates. The difference of the energies grew when the size of the system was increased. As the eigenstates of lowest energy correspond to the ground states of the SK model and the cycles of lowest energy correspond to the ground states of the symmetric Little model, we then considered the possibility that, in the thermodynamic limit, the free energy of the SK model might be larger than the free energy of the symmetric Little model. In the replica-symmetric approximation, the same energy was found in the context of neural networks.[4] The question concerning a possible difference between these energies when the replica symmetry is broken remained open.

Since the symmetric Little model is analytically more complex than the asymmetric one, and since our main interest is the study of static properties, we have concentrated on the asymmetric case which simplifies considerably the analysis. In fact, similar behavior is found in the symmetric and the asymmetric cases at low temperatures, as shown in Figs. 1(a) and 1(b). In Fig. 1(a), we plot the energies for the symmetric Little model with binary couplings i.e., at $T=0.5$, $J=\pm 1/\sqrt{N-1}$ vs $N^{-1/2}$. These results (as those shown in Ref. 1 at $T=0$) suggest that the energy of the symmetric Little model is clearly lower than that in the SK model. For small sizes, the difference between these energies increases as the size grows. If we were to extrapolate the energy of the Little model to the limit $N\to\infty$ by a straight line, as is sometimes done[5] for the SK model, we would obtain different values. On the other hand, in Fig. 1(b) we plot the energies of the asymmetric Little model and the SK model for the case of Gaussian couplings [zero mean and $1/(N-1)$ variance] at $T=0.5$ vs $N^{-1/2}$. As happens for the data shown in Fig. 1(a) for the symmetric Little model, the energy of the asymmetric case is also lower than that in the SK model.

It has to be pointed out that the differences in energy between the Little model (both symmetric and asymmetric cases) and the SK model for small sizes is strongly dependent on the nature of the distribution of couplings (if it is binary or Gaussian and if their variances behaves like $1/N$ or $1/N-1$). For instance, the analog of Fig. 1(b) for the asymmetric Little model, but using binary couplings instead of Gaussian ones, shows that both models seem to converge to the same value of energy in the thermodynamic limit. Since the different distribution of

couplings introduce $1/N$ corrections to all the thermodynamic quantities, we are led to the conclusion that only a systematic study (theoretical and also numerical for large sizes) will shed light on these questions. Even though this task could be undertaken for the Little model in the symmetric case, we have focused our study in the asymmetric one.

In fact, all features and conclusions of this work are common to both models. In many aspects (the formulation of the problem, the mathematical structure of the formulas, and the procedure to follow in solving it), when solving the asymmetric Little model we are facing the same type of questions as in the symmetric case but with greater simplicity. This gives us confidence that the main features for the asymmetric Little model can be extended to the symmetric case. In fact, in our original investigation we looked for the symmetric Little model. When solving the symmetric Little model by means of the replica method, one arrives at a saddle-point equation in an order-parameter space consisting of four matrices and one vector. The order-parameter space is too much large

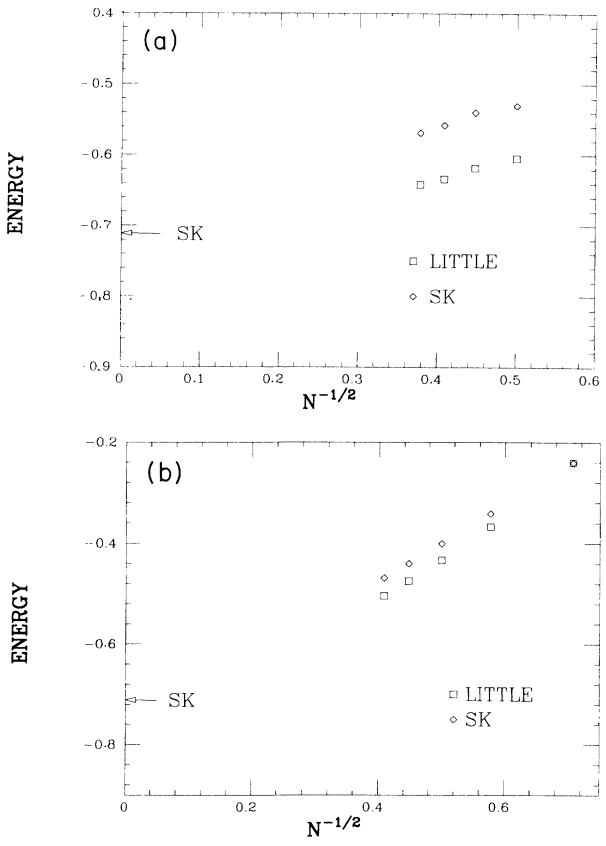

FIG. 1. (a) Energy for the symmetric Little model and the SK model plotted vs $N^{-1/2}$ by making exact calculations of the partition function for small samples at $T=0.5$. Analog results at $T=0$ are shown in Ref. 1. It seems that $f_{\rm LIT} \leq f_{\rm SK}$, signaling the possibility of a different behavior between both models. (b) Energy for the asymmetric Little model and the SK model plotted vs $N^{-1/2}$ by making exact calculations of the partition function for small samples at $T=0.5$. It seems that $f_{\rm LIT} \leq f_{\rm SK}$, signaling the possibility of a different behavior between both models.

to perform reliable calculations. Moreover, if the symmetric Little model coincides with the SK model, further study of the spectrum of fluctuations in order to compute finite-size effects can be very cumbersome. On the other hand, in case of the asymmetric Little model, one arrives to a problem in which the only order parameters are two matrices which reduce considerably the complexity of the analysis. Then, a lot of simplicity is gained.

To substantiate the main idea on the similarity of the results between the symmetric Little model and the asymmetric Little model, we present in Sec. VI numerical results for the symmetric case. They confirm our predictions and strengthen our conclusions.

From now on, when we speak about the Little model we are implicitily assuming that we are treating the asymmetric case. In this work we will corroborate a result already suggested in earlier works, i.e., the Little model converges to the SK model in the thermodynamic limit. We will explain how the finite-size behavior of the Little model, which led us to suspect the possible existence of different thermodynamic limits for these models, can be understood.

The paper is organized as follows. In Sec. II, we solve the model by using the standard techniques of spin-glass theory. We introduce some order parameters and we show some peculiar features in their solutions. In Sec. III, we will study and prove the stability of the SK-like solution for the Little model. In Sec. IV, we will compute the main finite-size corrections for the difference of free energy between the Little model and the SK model and we will see that it goes as $1/N$. In Sec. V, we will obtain the main finite-size corrections for an interesting order parameter which vanishes with a $1/N$ correction. These results will clearly show that the SK solution is the correct one (the stable solution of lowest free energy) for the Little model. Numerical results will be presented in Secs. IV and V in order to test the theoretical predictions. In Sec. VI, we present numerical results on the symmetric Little model in the same line as presented in Secs. IV and V. They strengthen the main ideas of our work. Section VII summarizes the results. Some comments on finite-size corrections for the SK model in the spin-glass phase will be in order.

II. ANALYTICAL SOLUTION OF THE LITTLE MODEL

In this section we proceed in order to solve the asymmetric Little model defined in Eq. (1). Applying the replica technique[6] and using standard procedures for spin glasses,[7] we obtain the following saddle-point equation:

$$\overline{Z_J^n} = \int \prod_{a<b} \left[\left(\frac{N\beta^2}{\pi} \right) dP_{ab} dQ_{ab} \right] \exp[-NA(P,Q)] , \tag{2}$$

where

$$A(P,Q) = -\frac{\beta^2 n}{2} + \beta^2 \sum_{a<b} (P_{ab}^2 + Q_{ab}^2) - \ln \mathrm{Tr}_\sigma \exp\left[\beta^2 \sum_{a<b} (P_{ab} + iQ_{ab}) \sigma_a \sigma_b \right] - \ln \mathrm{Tr}_\tau \exp\left[\beta^2 \sum_{a<b} (P_{ab} - iQ_{ab}) \tau_a \tau_b \right] \tag{3}$$

and

$$P_{ab}=-\tfrac{1}{2}(\langle\sigma_a\sigma_b\rangle+\langle\tau_a\tau_b\rangle)\,,$$
$$Q_{ab}=-\frac{i}{2}(\langle\sigma_a\sigma_b\rangle-\langle\tau_a\tau_b\rangle)\,, \tag{4}$$

with

$$\langle\sigma_a\sigma_b\rangle=\frac{\mathrm{Tr}_\sigma\sigma_a\sigma_b\exp\left[\beta^2\sum_{a<b}(P_{ab}+iQ_{ab})\sigma_a\sigma_b\right]}{\mathrm{Tr}_\sigma\exp\left[\beta^2\sum_{a<b}(P_{ab}+iQ_{ab})\sigma_a\sigma_b\right]}\,, \tag{5}$$

$$\langle\tau_a\tau_b\rangle=\frac{\mathrm{Tr}_\tau\tau_a\tau_b\exp\left[\beta^2\sum_{a<b}(P_{ab}-iQ_{ab})\tau_a\tau_b\right]}{\mathrm{Tr}_\tau\exp\left[\beta^2\sum_{a<b}(P_{ab}-iQ_{ab})\tau_a\tau_b\right]}\,. \tag{6}$$

We extract the free energy per spin making the usual analytic continuation:

$$f_{\mathrm{LIT}}=\lim_{n\to 0}\lim_{N\to\infty}\frac{\overline{Z_J^n}-1}{2Nn} \tag{7}$$

(the factor $2N$ comes when normalizing correctly the free energy in order to compare it with the free energy of the SK model).

The correct solution minimizes the free energy in the space of matrices P,Q. The usual SK solution is recovered if we suppose that the symmetry between σ and τ is not broken. That is, $\langle\sigma_a\sigma_b\rangle=\langle\tau_a\tau_b\rangle$ which means $P=P_{\mathrm{SK}}$ (which is the hierarchical parameterization for the SK model) and $Q=0$. On the contrary, if $Q\neq 0$ below a certain temperature, it would mean that the symmetry between σ and τ is broken and another phase transition is expected.

We can obtain several order parameters for the Little model depending on what correlation functions we consider. We want to show some peculiarities to take into account when solving the Little model because they will be of interest in Sec. IV. To this end, we introduce the following overlap:

$$q_A=\frac{1}{N}\sum_{i=1}^{N}\sigma_i^1\sigma_i^2\,. \tag{8}$$

It is the overlap between two sets of spins σ belonging to two different replicas. Averaging over all the phase space of configurations σ,τ $[\langle(\cdots)\rangle]$ and averaging over the disorder $[\overline{(\cdots)}]$, we obtain

$$\overline{\langle q_A^2\rangle}=\frac{1}{N}+\frac{1}{N^2}\sum_{\substack{i,j=1\\(i\neq j)}}^{N}\overline{\langle\sigma_i^2\sigma_i^2\sigma_j^1\sigma_j^2\rangle}$$
$$\sim\langle\sigma_a\sigma_b\rangle^2\ \text{ as } N\to\infty\,. \tag{9}$$

Now we have to sum over all transformations of the matrices P and Q which contribute equally to the saddle-point exponent. In the SK model, these transformations are all the permutations of the order-parameter matrix.[8] In our case one has to be careful because we have two order-parameter matrices P,Q and only certain permutations are allowed. To find these permutations we look at $A(P,Q)$ in formula (3) and search for all the permutations of the matrices P,Q which leave it invariant. Let us consider the two terms $\sum_{a<b}(P_{ab}^2+Q_{ab}^2)$ and $\ln\mathrm{Tr}_\sigma\exp\ [\cdots]+\ln\mathrm{Tr}_\sigma\exp[\cdots]$. The term $\ln\mathrm{Tr}_\sigma\exp[\cdots]+\ln\mathrm{Tr}_\tau\exp[\cdots]$ is invariant if we make an arbitrary permutation of the matrix P or a permutation of the matrix Q. That is, in terms of the indices of the matrices, we can change freely $\sigma_i\leftrightarrow\sigma_j$, $\tau_k\leftrightarrow\tau_l$. But the term $\sum_{a<b}(P_{ab}^2+Q_{ab}^2)$ is invariant only when permutations of the indices of σ and τ are done in such a way that the product $(P_{ab}+iQ_{ab})(P_{ab}-iQ_{ab})$ is invariant. Then, the permutation $\sigma_i\leftrightarrow\sigma_j$ implies the permutation $\tau_i\leftrightarrow\tau_j$. Another allowed transformation is that which changes $\sigma_i\leftrightarrow\tau_i$ for all i. These transformations generate all the equivalent saddle points which contribute to the saddle-point integral. Summarizing, the transformations in question are (1) $\sigma_i\leftrightarrow\sigma_j$, $\tau_i\leftrightarrow\tau_j$, $l\le i,j\le n$, and (2) $\sigma_i\leftrightarrow\tau_i$ all i.

To obtain the correct expression for the second moment $\langle q_A^2\rangle$ we perform the sum over all equivalent saddle points and we obtain

$$\langle q_A^2\rangle=\frac{1}{n(n-1)}\sum_{a<b}(\langle\sigma_a\sigma_b\rangle^2+\langle\tau_a\tau_b\rangle^2)$$
$$=\frac{2}{n(n-1)}\sum_{a<b}(P_{ab}^2-Q_{ab}^2)\,. \tag{10}$$

We can obtain, for the Little model, the Bray and Moore formula for the energy (proceeding as for the SK model[9]):

$$U=-\frac{\beta}{2}(1-\overline{\langle\sigma_i\tau_j\rangle^2})\,. \tag{11}$$

In this case

$$\overline{\langle\sigma_i\tau_j\rangle^2}=\langle\sigma_a\sigma_b\rangle\langle\tau_a\tau_b\rangle$$
$$=\text{sum over all saddle points}$$
$$=\frac{2}{n(n-1)}\sum_{a<b}\langle\sigma_a\sigma_b\rangle\langle\tau_a\tau_b\rangle$$
$$=\frac{2}{n(n-1)}\sum_{a<b}(P_{ab}-iQ_{ab})(P_{ab}+iQ_{ab})=\frac{2}{n(n-1)}\sum_{a<b}(P_{ab}^2+Q_{ab}^2)\,. \tag{12}$$

Then, the formula is

$$U=-\beta_2\left[1-\frac{2}{n(n-1)}\sum_{a<b}(P_{ab}^2+Q_{ab}^2)\right]. \quad (13)$$

If $Q=0$, $P=P_{\rm SK}$, the energy converges to the value found in the SK model. With this introductory discussion we can test the stability of the SK solution for the Little model and compute the most interesting finite-size corrections.

III. STABILITY OF THE SK SOLUTION FOR THE LITTLE MODEL

To see if the solution $P=P_{\rm SK}$, $Q=0$ is stable, we have to investigate the spectrum of fluctuations around it inside the space of matrices P,Q. One finds:

$$A[P,Q]=A_{\rm SK}[P]+\beta^2\delta P^T G\delta P+\beta^2\delta Q^T M\delta Q \quad (14)$$

(terms of the type $\delta P^T\delta Q$ are absent, which is not the case for the symmetric Little model), where $M=2-G$ and G is the de Almeida–Thouless stability matrix for the SK model:[10]

$$G_{(ab)(cd)}=\delta_{(ab)(cd)}-\beta^2(\langle\sigma_a\sigma_b\sigma_c\sigma_d\rangle-\langle\sigma_a\sigma_b\rangle\langle\sigma_c\sigma_d\rangle). \quad (15)$$

To get a stable solution, all the eigenvalues of the matrix G and M have to be non-negative. We already know that this is the case for the matrix G if the hierarchical solution[11,12] is the correct one for the SK model.[13] The crucial point refers to the matrix M. Does it have any negative eigenvalues?

Remaining near and below T_c, one can see very easily that $P=P_{\rm SK}$, $Q=0$ is a stable solution. If $Q=0$ is a stable solution in the spin-glass phase, the de Almeida–Thouless matrix has to satisfy $G\le 2$. This implies $\langle\sigma_a\sigma_b\sigma_c\sigma_d\rangle-\langle\sigma_a\sigma_b\rangle\langle\sigma_c\sigma_d\rangle$ to be positive definite, which seems to be some kind of "reversed" Schwarz inequality. This could be a consequence of the analytic continuation $n\to 0$.

Anyway, because it is needed to study finite-size corrections in the following section, we have obtained all the spectra of eigenvalues for the matrix M at zero and first order of replica-symmetry breaking to test the stability of the $Q=0$ solution. This is the same as finding the spectrum of eigenvalues for the matrix G (remember $M=2-G$). Our purpose is to look for the dangerous eigenvalues for the matrix M (the lowest eigenvalues of the spectrum) and to see if there is at least one of them which becomes negative. Since $M=2-G$, those sectors in replica space which can be unstable for M correspond to the most stable ones for the stability matrix G. The spectrum of eigenvalues for the matrix M is the following.

(1) Replica symmetric solution. The spectrum has three eigenvalues.[10] Two of them coincide in the limit $n\to 0$ (the anomalous and the longitudinal one). The behavior of the longitudinal anomalous eigenvalue (the most dangerous for the matrix M) is plotted in Fig. 2(a) in all the spin-glass phase.

(2) First order of replica-symmetry breaking. At this order, following the work of De Dominicis and Kondon,[14] we find a spectrum of 10 eigenvalues (2 longitudinals, 4 anomalous, and 4 replicas). We have not found in the literature an expression for the eigenvalues and their degeneracies. Since it could be of some interest to other people, we present our results in the Appendix.

In Fig. 2(b) we plot the three most unacceptable eigenvalues for the matrix M in the spin-glass phase (one belongs to the longitudinal spectrum, one to the anomalous, and the other to the replicon sector). Since it is difficult to solve numerically the eigenvalues for temperatures less than 0.1, data for this regime are lacking. Anyway an extrapolation of the data suggests that the eigenvalues are well behaved when the temperature goes to zero.

In both cases we find $M\ge 1$. This fact strongly suggests that this will be a general result at any step of replica-symmetry breaking. Then, we expect the SK

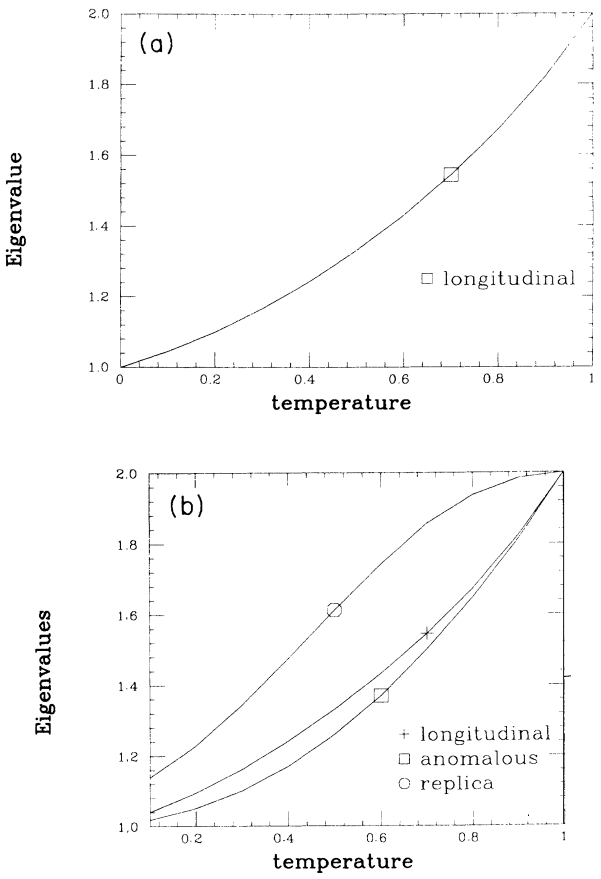

FIG. 2. (a) We plot the most unacceptable eigenvalue of the matrix M (the longitudinal anomalous) for the replica-symmetric case. The SK solution for the Little model is stable at this zeroth-order step. The eigenvalue is always positive and greater than 1 according to the "reversed" Schwarz inequality. (b) At first order of replica-symmetry breaking the matrix M gives a spectrum of 10 eigenvalues (2 longitudinals, 4 anomalous, and 4 replicons). We plot the three most unacceptable eigenvalues at a temperature greater than 0.1. The eigenvalues are all positive and greater than 1 indicating that the SK solution remains stable at this order of replica-symmetry breaking.

solution to be stable for the Little model. The following step will be to see whether the SK solution is the solution of lowest free energy for the Little model. The study of finite-size effects is a powerful tool to settle the question.

IV. FINITE-SIZE CORRECTIONS TO THE ENERGY

If we want to see numerically if the asymmetric Little model really converges to the SK model, it is not useful to look at properties as, for example, the energy. In fact, we cannot extrapolate to $N\to\infty$ numerical results for finite sizes because finite-size corrections are unknown even at the level of mean-field theory for spin glasses. In Fig. 3, we plot the energy of the Little model vs $N^{-1/2}$ at $T=0.5$ obtained by means of Monte Carlo numerical simulation (binary distribution of couplings with $1/N$ variance) and the theoretical prediction for the SK model at first order of replica-symmetry breaking (which is very near to the solution at infinite order of replica-symmetry breaking by a difference less than 10^{-3}). A polynomial fits the data well but we are not sure whether the finite-size effects behave as $N^{-1/2}$,[5] mainly because, for those sizes which would decide finally which is the main correction that controls the convergence, numerical simulations need too much CPU time (even though we have made use of a very efficient program). The error bars of the data, being of order 10^{-3}, are smaller than the size of the square symbols.

Now we want to obtain more precise information about the convergence of the Little model towards the SK model and we want to understand the nature of the finite-size corrections which could explain the results shown in Figs. 1(a) and 1(b). We already know that the finite-size corrections to the free energy of the SK model are by now an unsolved problem. What we can do is to look for magnitudes in which the main behavior is controlled by a finite-size correction of the type $1/N$. These corrections are easily tractable because they do not contain a complex spectrum of zero modes which are, in fact, the difficult point in computing finite-size corrections for the SK model. Now it is easy to understand what those magnitudes are that show this kind of finite-size correction. Since, when $Q=0$, we recover the SK model, we expect to find $1/N$ corrections for those magnitudes whose fluctuations are governed by the spectrum of modes in the space of Q matrices, i.e., fluctuations given by the stability matrix M introduced in the last section.

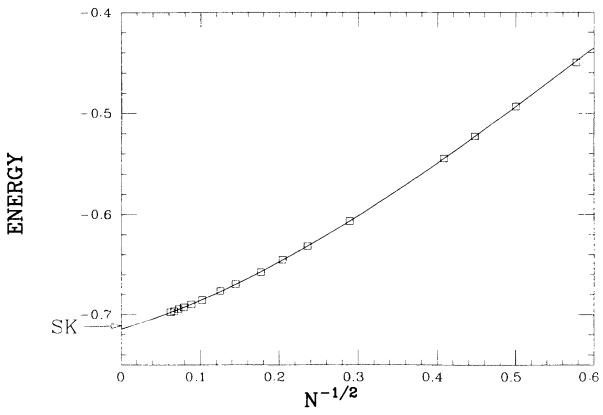

FIG. 3. Energy for the asymmetric Little model for different sized plotted vs $N^{-1/2}$ at $T=0.5$. We find the usual finite-size corrections as in the SK model. A polynomial fits the data very well and converges towards the expected result for the SK model $U\simeq -0.711$ at infinite order of replica-symmetry breaking. By looking at this figure, one is tempted to say that the dominant corrections behave as $N^{-1/2}$.

In this work we study the behavior of two quantities.

(1) The first one is the difference between the free energies of the Little model and the SK model. Even though we do not know which is the main finite-size correction to each one of these magnitudes, its difference goes like $1/N$ since fluctuations are governed by the stability matrix M. Higher-order corrections become confusing and it is not clear how the series proceeds at higher orders. We speculate about powers of $N^{-1/2}$.

(2) The second one is an overlap proportional to $\sum_{a<b}Q_{ab}^2$ which is nonzero if the symmetry between the spins σ and τ is broken. We will show that this term goes to zero in the limit $N\to\infty$ with a main finite-size correction of the type $1/N$ (also in this case, the spectrum of fluctuations around the solution $Q=0$ is given by the stability matrix M).

To study the energy, the first thing which we have to take into account is that there are many factors which affect the $1/N$ correction in a spin glass. For example, we can consider for the SK model a distribution of binary or Gaussian couplings with zero mean and variance $1/N$. Even though in both cases the thermodynamic limit is the same, $1/N$ corrections are strongly dependent on the choice. Since we want to compare our theoretical prediction with numerical simulations, we have to take into account, in the theoretical treatment, what the probability distribution of couplings is that we are going to implement in the Monte Carlo simulation.

Because it is computationally faster, we have considered the case of a binary distribution of couplings:

$$P(J_{ij})=\tfrac{1}{2}[\delta(J_{ij}+J)+\delta(J_{ij}-J)] \tag{16}$$

with $J=1/\sqrt{N}$. We have to proceed step by step and to add all different contributions of order $1/N$.

Let us begin by studying the asymmetric Little model with a Gaussian distribution of couplings:

$$P(J_{ij})=\left[\frac{N}{2\pi}\right]^{1/2}\exp\left[\frac{-NJ_{ij}^2}{2}\right]. \tag{17}$$

After, we will consider the correction due to the fact that we are using binary couplings.

In this case, if we do not neglect corrections of order $1/N$, we arrive at a saddle-point expression [similar to Eq. (2)]:

$$\overline{Z_J^n(G)}=\exp\left[\frac{-\beta^2 n}{2}\right]\int\prod_{a<b}\left[\left[\frac{N\beta^2}{\pi}\right]dP_{ab}\,dQ_{ab}\right]\times\exp[-NA(P,Q)], \tag{18}$$

where G stands for Gaussian and

$$A(P,Q)=-\frac{\beta^2 n}{2}+\beta^2\sum_{a<b}(P_{ab}^2+Q_{ab}^2) - \ln \mathrm{Tr}_{\{\sigma\tau\}}\exp[C(P,Q)] \tag{19}$$

with

$$C(P,Q)=\beta^2\sum_{a<b}(P_{ab}+iQ_{ab})\sigma_a\sigma_b +\beta^2\sum_{a<b}(P_{ab}-iQ_{ab})\tau_a\tau_b -\frac{\beta^2}{N}\sum_{a<b}\sigma_a\sigma_b\tau_a\tau_b \ . \tag{20}$$

If we expand the term $(1/N)\sum_{a<b}\sigma_a\sigma_b\tau_a\tau_b$, we get

$$\overline{Z_J^n(G)}=\exp\left[\frac{-\beta^2 n}{2}\right]\int\prod_{a<b}\left[\left[\frac{N\beta^2}{\pi}\right]dP_{ab}dQ_{ab}\right] \times\exp[-NA_0(P,Q)] \times g(P,Q) \tag{21}$$

with

$$g(P,Q)=\left[1-\frac{\beta^2}{N}\sum_{a<b}\langle\sigma_a\sigma_b\tau_a\tau_b\rangle+O\left[\frac{1}{N^2}\right]\right]^N \tag{22}$$

and

$$A_0(P,Q)=-\frac{\beta^2 n}{2}+\beta^2\sum_{a<b}(P_{ab}^2+Q_{ab}^2)-\ln Z \ , \tag{23}$$

where Z is given by

$$Z=\mathrm{Tr}_{\{\sigma\tau\}}\exp\left[\beta^2\sum_{a<b}(P_{ab}+iQ_{ab})\sigma_a\sigma_b +\beta^2\sum_{a<b}(P_{ab}-iQ_{ab})\tau_a\tau_b\right] \tag{24}$$

and the angular brackets mean

$$\langle(\cdots)\rangle=\frac{\mathrm{Tr}_{\sigma\tau}(\cdots)\exp\left[\beta^2\sum_{a<b}[(P_{ab}+iQ_{ab})\sigma_a\sigma_b+(P_{ab}-iQ_{ab})\tau_a\tau_g]\right]}{\mathrm{Tr}_{\sigma\tau}\exp\left[\beta^2\sum_{a<b}[(P_{ab}+iQ_{ab})\sigma_a\sigma_b+(P_{ab}-iQ_{ab})\tau_a\tau_b]\right]} \ . \tag{25}$$

But

$$\sum_{a<b}\langle\sigma_a\sigma_b\tau_a\tau_b\rangle=\sum_{a<b}\langle\sigma_a\sigma_b\rangle^2+O(1/N) \tag{26}$$

as we will see in the next section [in fact, $\langle\sigma_a\sigma_b\tau_a\tau_b\rangle=\langle\sigma_a\sigma_b\rangle\langle\tau_a\tau_b\rangle$ and we will show that $\sum_{a<b}\langle\sigma_a\sigma_b-\tau_a\tau_b\rangle^2\simeq O(1/N)$].

We get the expression

$$f_{\mathrm{LIT}}^G(N)=-\frac{1}{2N\beta n}\ln[\overline{Z_J^n(G)}] =\frac{\beta}{4N}\left[1-\frac{2}{n(n-1)}\sum_{a<b}\langle\sigma_a\sigma_b\rangle^2\right]-\frac{1}{2N\beta n}\ln\int\prod_{a<b}\left[\left[\frac{N\beta^2}{\pi}\right]dP_{ab}dQ_{ab}\right]\exp[-NA_0(P,Q)] \ . \tag{27}$$

Now we expand $A_0(P,Q)$ around the stable solution $Q=0$:

$$A_0(P,Q)=A_{\mathrm{SK}}(P)+\beta^2 Q^T M Q+O(Q^4) \ , \tag{28}$$

where

$$A_{\mathrm{SK}}(P)=-\frac{\beta^2 n}{2}+\beta^2\sum_{a<b}P_{ab}^2 -2\ln\mathrm{Tr}_\sigma\exp\left[\beta^2\sum_{a<b}P_{ab}\sigma_a\sigma_b\right] \tag{29}$$

and $M=2-G$ is the stability matrix quoted before.

Performing the Gaussian integral over Q, we finally obtain

$$f_{\mathrm{LIT}}^G(N)=-\frac{1}{2N\beta n}\ln\int\prod_{a<b}\left[\left[\frac{N\beta^2}{\pi}\right]^{1/2}dP_{ab}\right] \times\exp[-NA_{\mathrm{SK}}(P,Q)] -\frac{U_{\mathrm{SK}}}{2N}+\frac{\ln(\det M)}{4\beta Nn} +(\text{higher-order terms}) \ . \tag{30}$$

The first term in the rhs is nothing else but the normalized free energy of the SK model with $2N$ spins and we obtain the desired result

$$f_{\mathrm{LIT}}^G(N)-f_{\mathrm{SK}}^G(2N)=-\frac{U_{\mathrm{SK}}}{2N}+\frac{\ln(\det M)}{4\beta nN} +(\text{higher-order terms}) \ . \tag{31}$$

By high-order terms we mean unknown finite-size corrections which decrease faster than $1/N$. Since we are working with binary couplings, we want to obtain the finite-size correction to the free energy of the Little model when considering binary couplings versus Gaussian ones.

This factor is easy to obtain. In fact, for the binary case we have

$$\overline{Z_J^n(B)}=\mathrm{Tr}_{\{\sigma\tau\}}\left\{\prod_{i\neq j}\cosh\left[\frac{\beta}{N^{1/2}}\left[\sum_a \sigma_i^a\tau_j^a\right]\right]\right\}, \tag{32}$$

where B stands for binary. Expanding the hyperbolic cosine, we obtain the first-order correction

$$\cosh\left[\frac{\beta}{N^{1/2}}\left[\sum_a \sigma_i^a\tau_j^a\right]\right]=\exp\left[\frac{\beta^2}{2N}\left[\sum_a \sigma_i^a\tau_j^a\right]\right]\left[1-\frac{\beta^4}{12N^2}\left[\sum_a \sigma_i^a\tau_j^a\right]^4\right],$$

$$\overline{Z_J^n(B)}=Z_J^n(G)\left[1-\frac{\beta^4}{12N^2}\sum_{i\neq j}\left\langle\left[\sum_a \sigma_i^a\tau_j^a\right]^4\right\rangle_G\right], \tag{33}$$

$$f_{\mathrm{LIT}}^B(N)=f_{\mathrm{LIT}}^G(N)-\frac{1}{2\beta Nn}\ln\left[1-\frac{\beta^4}{12N^2}\sum_{i\neq j}\left\langle\left[\sum_a \sigma_i^a\tau_j^a\right]^4\right\rangle_G\right],$$

where $\langle\cdots\rangle_G$ means the average over the weight given by $Z_J^n(G)$.

We obtain

$$f_{\mathrm{LIT}}^G(N)=f_{\mathrm{LIT}}^B(N)=\frac{\alpha}{N}+(\text{higher-order terms}), \tag{34}$$

$$\alpha=\frac{\beta^3}{24}\left[2+\frac{8}{n}\sum_{(ab)}\langle\sigma_a\sigma_b\rangle^2-\frac{1}{n}\sum_{(abcd)}\langle\sigma_a\sigma_b\sigma_c\sigma_d\rangle^2\right], \tag{35}$$

and the sums run over different replica indices.

The same expression can be obtained for the SK model:

$$f_{\mathrm{SK}}^B(N)-f_{\mathrm{SK}}^B(N)=\frac{\alpha}{N}+(\text{higher-order terms}). \tag{36}$$

Combining formulas (31), (34), and (36), we obtain

$$f_{\mathrm{LIT}}^B(N)-f_{\mathrm{SK}}^B(2N)=\frac{\lambda}{N}+(\text{high-order terms}) \tag{37}$$

with

$$\lambda=\frac{1}{4\beta n}\ln(\det M)-\left[\frac{\alpha+U_{\mathrm{SK}}}{2}\right], \tag{38}$$

and, for the internal energy,

$$U_{\mathrm{LIT}}^B(N)-U_{\mathrm{SK}}^B(2N)=\frac{a}{N}+(\text{higher-order terms}) \tag{39}$$

with $a=\partial(\beta\lambda)/\partial\beta$.

Now we can understand the results shown in Figs. 1(a) and 1(b). There we plot $U_{\mathrm{SK}}^B(N)$ and $U_{\mathrm{LIT}}^B(N)$ and we see how their difference behaves as N grows. This difference does not behave purely as $1/N$ since one should compare the Little model with the SK model, the last with a double number of spins.

If we suppose (as seems to be the case, at least for small sizes) that all the thermodynamic quantities (U_{SK}, $\sum_{(ab)}\langle\sigma_a\sigma_b\rangle^2$, $\sum_{(abcd)}\langle\sigma_a\sigma_b\sigma_c\sigma_d\rangle^2$, $\sum_{(ab)}\langle\sigma_a\sigma_b\tau_a\tau_b\rangle$,...) have finite-size corrections like powers of $N^{-1/2}$, then

$$\delta U=U_{\mathrm{LIT}}^B(N)-U_{\mathrm{SK}}^B(2N)=\frac{a}{N}+\frac{b}{N^{3/2}}+\frac{c}{N^2}+O\left[\frac{1}{N^{5/2}}\right] \tag{40}$$

and

$$N\,\delta U=a+\frac{b}{N^{1/2}}+\frac{c}{N}+O\left[\frac{1}{N^{3/2}}\right]. \tag{41}$$

One hopes that $N\,\delta U$ will be a polynomial in terms of $N^{-1/2}$. At $T=0.5$, in the spin-glass phase, we obtain from (37)

$$\begin{aligned} a&=0.0998\ \ (\text{RS case}),\\ a&=0.1053\ \ (\text{first-order RSB}). \end{aligned} \tag{42}$$

At infinite order of replica-symmetry breaking (RSB), we expect to obtain a value of a near 0.106. In fact, this magnitude only depends on extensive quantities like, for instance, the energy. At least for $T=0.5$ its variation will be less than 10^{-3} if we compute it at infinite order of replica-symmetry breaking in respect to the value we would obtain at first order of replica-symmetry breaking.

To test the correctness of our prediction, we plot in Fig. 4 the results obtained from Monte Carlo numerical simulations. As we said before, we have performed the numerical simulations for the case of binary couplings and variance $1/N$. The first four points, without error bars, are obtained by evaluating exactly the partition function for small systems $N=3,4,5,6$ [these results are different form those shown in Fig. 1(b) in which the distribution of couplings was Gaussian and not binary]. The other points have been obtained by Monte Carlo simulation for $N=12,18,24,32,48,64,96,128,256$ and a number of samples which varies from 3000 to 6000. We cannot go to larger sizes because the error bars are as large as the finite-size correction we want to compute. It is very difficult to reduce the size of the error bars because it would be take too much CPU time. Anyway, our results seem to be in agreement with the predicted result for $N\to\infty$.

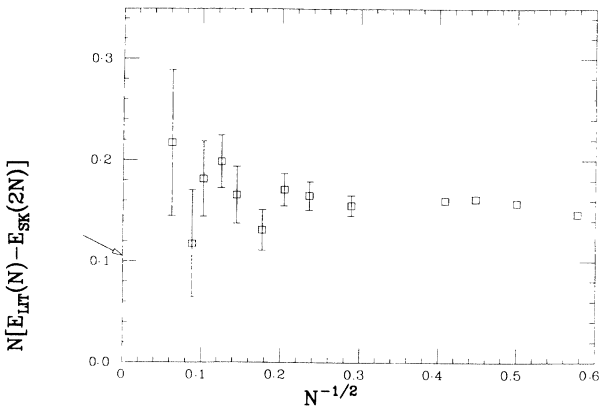

FIG. 4. $N\,\delta U$ (as defined in the text) plotted vs $N^{-1/2}$. It should converge towards $\simeq 0.105$ (the point indicated by an arrow). Since numerical error bars are as large as the finite-size correction, it is very difficult to predict with precision the value of a. The points without error bars are obtained by exact calculation of the partition function.

Looking at the results shown in Fig. 4, one is led to the conclusion that the difference of energy between the Little model and SK model decreases monotonically as we increase the size. This does not seem to be the case for the data shown in Fig. 1(b) where the distance does not decrease monotonically (in the case of results like those shown in Fig. 1(b) for a distribution of binary couplings, this difference would decrease much more slowly than we would infer from looking at Fig. 4). This is due to the fact that, in Figs. 1(a) and 1(b), we plot the energies for the Little and the SK models with an equal number of spins. On the contrary, in Fig. 4 we are comparing the energy of the Little model for N spins with the energy of the SK model with $2N$ spins. In fact, if we plotted the differences of energies shown in Figs. 1(a) and 1(b) vs $N^{-1/2}$, we would not find a $1/N$ behavior but corrections which decrease slower, for instance, like $N^{-\alpha}$ with $\alpha < 1$.

V. FINITE-SIZE CORRECTIONS TO AN OVERLAP

Let us now analyze how the term $\sum_{(ab)} Q_{ab}^2$ behaves as we make $N \to \infty$. We define two overlaps:

$$q_A = \frac{1}{N} \sum_{i=1}^{N} \sigma_i^1 \sigma_i^2 , \tag{43}$$

$$q_B = \frac{1}{2N} \left[\sum_{i=1}^{N} \sigma_i^1 \sigma_i^2 + \sum_{i=1}^{N} \tau_i^1 \tau_i^2 \right] . \tag{44}$$

We want to find what the behavior is of the difference of the squared overlaps $\delta q = \langle q_A^2 \rangle - \langle q_B^2 \rangle$ which can be directly computed by means of a Monte Carlo simulation. It is trivial to obtain

$$\begin{aligned} \delta_q &= \frac{1}{2N} \left[1 - \frac{2}{n(n-1)} \sum_{a<b} \langle \sigma_a \sigma_b \rangle^2 \right] \\ &\quad + \frac{N-1}{2N} \frac{1}{n(n-1)} \sum_{a<b} \langle \sigma_a \sigma_b - \tau_a \tau_b \rangle^2 \\ &= -\frac{U_{\mathrm{SK}}}{N\beta} + \frac{N-1}{2N} \frac{1}{n(n-1)} \sum_{a<b} \langle \sigma_a \sigma_b - \tau_a \tau_b \rangle^2 . \end{aligned} \tag{45}$$

We compute the second term of the rhs

$$\sum_{a<b} \langle \sigma_a \sigma_b - \tau_a \tau_b \rangle^2 = \frac{\int \prod_{a<b} [(N\beta^2/\pi) dP_{ab} dQ_{ab}] \exp[-NA(P,Q)] f(P,Q)}{\int \prod_{a<b} [(N\beta^2/\pi) dP_{ab} dQ_{ab}] \exp[-NA(P,Q)]} \tag{46}$$

with

$$f(P,Q) = \sum_{a<b} \left[\frac{\mathrm{Tr}_{\sigma\tau} (\sigma_a \sigma_b - \tau_a \tau_b) \exp[C(P,Q)]}{\mathrm{Tr}_{\sigma\tau} \exp[C(P,Q)]} \right]^2 \tag{47}$$

and

$$\begin{aligned} C(P,Q) &= \beta^2 \sum_{a<b} (P_{ab} + iQ_{ab}) \sigma_a \sigma_b \\ &\quad + \beta^2 \sum_{a<b} (P_{ab} - iQ_{ab}) \tau_a \tau_b \\ &\quad - \frac{\beta^2}{N} \sum_{a<b} \sigma_a \sigma_b \tau_a \tau_b . \end{aligned} \tag{48}$$

We expand $f(P,Q)$ around $Q = 0$:

$$f(P,Q) = -4/\beta^4 \sum_{a<b} (BQ)_{(ab)}^2 = -4\beta^4 Q^T B^2 Q , \tag{49}$$

where

$$B_{(ab)(cd)} = \langle \sigma_a \sigma_b \sigma_c \sigma_c \rangle - \langle \sigma_a \sigma_b \rangle \langle \sigma_c \sigma_d \rangle \tag{50}$$

and Q is a vector with components $Q_{(ab)}$. We have to compute

$$\sum_{a<b} \langle \sigma_a \sigma_b - \tau_a \tau_b \rangle^2 = \frac{-4\beta^4 \int d\bar{Q}\, Q^T B^2 Q}{\int d\bar{Q}} \tag{51}$$

with the measure

$$d\bar{Q} = \prod_{a<b} \left[\left(\frac{N\beta^2}{\pi} \right)^{1/2} dQ_{ab} \right] \exp[-N\beta^2 Q^T M Q] \tag{52}$$

and $M = I + \beta^2 B$ is the usual stability matrix studied in Sec. III. Making an orthogonal transformation, we diagonalize simultaneously B and M and we can perform very easily the Gaussian integrals:

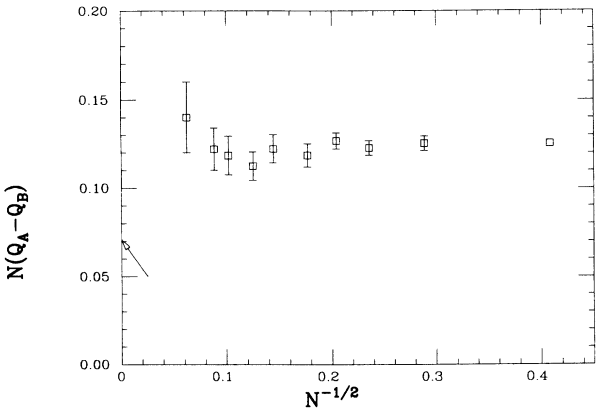

FIG. 5. $N\,\delta q$ (as defined in the text) plotted vs $N^{-1/2}$. It should converge towards $\simeq 0.0707$ (the point indicated by an arrow). The prediction seems to be in agreement with the data.

$$\sum_{a<b} \langle \sigma_a \sigma_b - \tau_a \tau_b \rangle^2 = -\frac{2\beta^2}{N} \mathrm{Tr}\left[\frac{B^2}{M}\right] + (\text{higher-order terms}) . \quad (53)$$

We substitute in (45)

$$\overline{\langle q_A^2 \rangle} - \overline{\langle q_B^2 \rangle} = \delta q = \frac{\gamma}{N} + (\text{higher-order terms}) \quad (54)$$

with

$$\gamma = -\frac{U_{\mathrm{SK}}}{\beta} + \frac{\beta^2}{n} \mathrm{Tr}\left[\frac{B^2}{M}\right] . \quad (55)$$

For $T=0.5$ we obtain the results

$$\begin{aligned} &\gamma = 8.52 \times 10^{-2} \ \text{(RS case)} , \\ &\gamma = 7.077 \times 10^{-2} \ \text{(first-order RSB)} . \end{aligned} \quad (56)$$

If we want to know what the value of γ is at infinite order of replica-symmetry breaking, the same observations which we made in the last section apply in this case. Similarly, as we made before for the energy, we can suppose that the higher-order corrections behave as powers of $N^{-1/2}$. We should see a polynomial behavior of $N\delta q$ when plotted vs $N^{-1/2}$. Figure 5 shows the results obtained by making numerical simulations for several sizes ($N=6,12,18,14,32,48,64,96,128,256$ and a number of samples which varies from 3000 to 6000). Now, we find a slow convergence towards the expected result which is affected by higher-order corrections.

VI. NUMERICAL RESULTS FOR THE SYMMETRIC LITTLE MODEL

In order to substantiate our ideas and to strengthen the main conclusions of this work, numerical results are presented for the symmetric Little model. As was said in the Introduction, when studying the symmetric Little model by means of the replica technique, we arrive at a saddle-point equation depending on four matrices and one vector. The SK solution is recovered in the special case in which two of these matrices vanish (which corresponds to the case in which the symmetry $\sigma_i \leftrightarrow \tau_i$ is not broken). Even though we agree that, for the symmetric Little model, the complexity of the order-parameter space further complicates the theoretical analysis, we think that the same features as in the asymmetric Little model are valid in this case.

We have performed Monte Carlo numerical simulations for the symmetric Little model (as in the asymmetric case, we have used a binary distribution of couplings with $1/N$ variance) at $T=0.5$. In Fig. 6, we show a plot of the internal energy of the symmetric Little model versus size (we have explored sizes from $N=18$ to 640 spins). It is now compatible with an $N^{-1/2}$ behavior (even though we should say that $N^{-2/3}$ corrections fit the numerical data better). Now, as in Fig. 3, the error bars are of the size of the square marks.

Figures 7 and 8 show the same kind of results as have been plotted in Fig. 4 and 5. Data are available from $N=18$ to 256 with a number of samples which vary between 2000 and 10 000. All simulations have also been performed in the middle of the spin-glass phase at $T=0.5$. The points where the error bars have not been plotted are because they are smaller than the size of the square symbols.

In Fig. 7 we show the difference of the internal energy between the symmetric Little model with N spins and that of the SK model with $2N$ spins. This difference goes like $1/N$ as was expected. Nevertheless, for the symmetric Little model, the expression $N[E_{\mathrm{LIT}}(N) - E_{\mathrm{SK}}(2N)]$ tends to a negative value instead of a positive one like that found in the asymmetric Little model.

In Fig. 8 we plot the order parameter $N\,\delta q$ as defined in Eq. (54). This is the corresponding plot of that shown in Fig. 5 and curiously similar values for $N\,\delta q$ seem to be obtained as in the asymmetric case. The $1/N$ behavior is confirmed and δq vanishes in the thermodynamic limit (which means that the symmetric Little model converges to the SK model).

Some comments concerning the error bars in this last

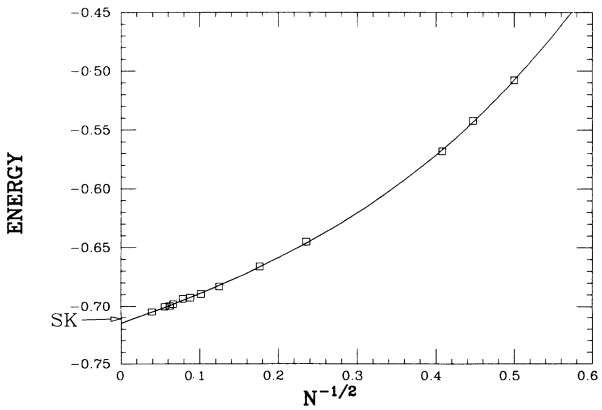

FIG. 6. Energy for the symmetric Little model for different sizes plotted vs $N^{-1/2}$ at $T=0.5$. The size of the error bars are smaller than the size of the square symbols.

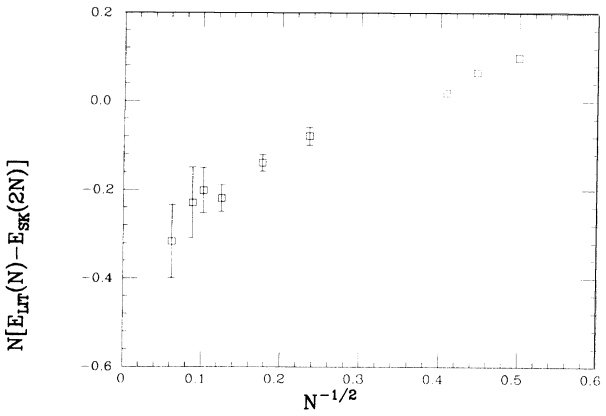

FIG. 7. $N\,\delta U$ (as in Fig. 4) plotted vs $N^{-1/2}$ for the symmetric Little model. The points without error bars are obtained by means of exact calculation of the partition function.

plot are in order. Since the plotted magnitude $N\,\delta q$ is the difference of two quantities, we could obtain the size of the error bars by means of the triangular law (if the size of the error bars for both overlaps q_A and q_B are the cateta of a rectangular triangle, then the size of the error bar for the difference is represented by the hypothenusa of the same triangle). This result supposes that both overlaps q_A and q_B are uncorrelated. This is not the case for the Little model (in the symmetric or asymmetric cases). Nevertheless, for the symmetric case, the correlation between q_A and q_B for one sample is expected to be greater than in the asymmetric case because, in the symmetric case, each spin σ sees the same local field as each spin τ due to the fact that the coupling matrix J_{ij} is symmetric. In fact, the simulations show that the size of the error bars for the quantity $N\,\delta q$ in the symmetric case are approximately three times smaller than in the asymmetric case.

It would be interesting to test our numerical results shown in Figs. 7 and 8 against theoretical predictions for the symmetric Little model. The numerical predictions would be safer in this case because the error bars are neatly smaller than in the asymmetric case. We think that these last plots clarify the question about the thermodynamic behavior of the symmetric Little model at infinite order of replica-symmetry breaking.

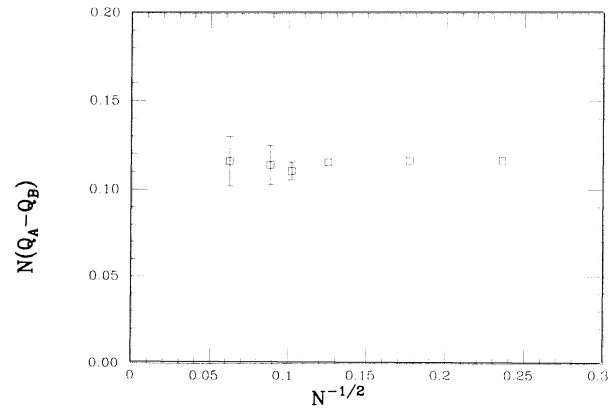

FIG. 8. $N\,\delta q$ (as in Fig. 5) plotted vs $N^{-1/2}$ for the symmetric Little model. The size of the error bars is smaller than the size of the square symbols. It seems to be constant over the studied range of sizes.

VII. CONCLUSIONS

In this work we have proved, by a stability analysis and a study of the finite-size corrections, that the asymmetric Little model converges to the SK model in the thermodynamic limit. We have shown that the SK solution is stable for the Little model. Then, to be sure that this is really the stable solution of minimum free energy, we have performed a study of the finite-size corrections. We have discovered that the free-energy difference between the Little model and the SK model, the latter with a double number of spins, behaves as $1/N$ plus nontrivial high-order terms. Our theoretical prediction is compatible with the data obtained from numerical simulations. By constructing a difference of two overlaps, we have shown that its main finite-size corrections also behave as $1/N$. For both magnitudes we find a convergence compatible with the one we expect to be the correct result. However, large error bars do not allow us to predict the value as $N\to\infty$. The same conclusions are achieved by performing numerical studies for the symmetric Little model. The theoretical analysis, following the same lines as in the asymmetric case, is expected to yield the same results.

Two observations can be made by looking at Figs. 4 and 5. Since $N\,\delta U$ tends to a finite value as $N\to\infty$, it means that $\delta U\to 0$ and the Little model have the same energy as the SK model in the thermodynamic limit. Also, since $N\delta q$ tends to a finite value when $N\to\infty$, we see that $\sum_{(ab)}Q_{ab}^2$ (which is $\sum_{a<b}\langle\sigma_a\sigma_g-\tau_a\tau_b\rangle^2$) goes to zero in the thermodynamic limit. That is, $Q=0$ and $P=P_{\rm SK}$ is the correct stable solution for the asymmetric Little model.

The second observation refers to the nature of the aforementioned high-order terms. From our data, we cannot say what the main behavior of these corrections is. In Figs. 4 and 5, we find that the plotted magnitudes could be accounted for by a power-law behavior of the type $N^{-\alpha}$, but it is not possible to decide on the value of α. It is important to observe that these high-order corrections are a "mass" of factors all emerging from the spectrum of zero modes which are present in the spin-glass phase. It should be interesting to perform an extensive study (at a theoretical or numerical level) of what the nature of the finite-size corrections is for the SK model. There are some hints in the literature which point towards finite-size corrections for self-averaging quantities of a power-law type $N^{-1/2}$.[15,5] But these studies, sometimes done for small systems and a large number of samples or large systems but a small number of samples, have not yet been able to decide the question. The situation worsens when one notes the fact that we do not have any theoretical prediction. In our work, we have supposed for α the value $\frac{1}{2}$. However, we do not have any convinc-

ing reason to discard other values. In fact, we have found the exponent $\alpha=\frac{2}{3}$ to be compatible with the results shown in the Figs. 3 and 6. For us, this is an interesting open question which merits further investigation along this line.

We have also done extensive numerical simulations for the symmetric Little model which suggest that the results we have shown for the asymmetric Little model are also valid for the symmetric case. In the symmetric case the error bars are smaller and it could be interesting to test the numerical results presented here against theoretical predictions. The theoretical study of the symmetric case presents more technical difficulties because the spectrum of fluctuations around the SK solution is more complex but we think that the main physics and the nature of the finite-size corrections will follow the same lines as in the asymmetric case.

ACKNOWLEDGMENTS

We acknowledge stimulating discussions with F. Slanina, L. Biferale, S. Franz, and the interesting suggestions of I. Kondor. One of us (F.R.) acknowledges the Ministerio de Educación y Ciencia in Spain (PN89-46230540) for partial support. One of us (G.P.) was supported in part by I.N.F.N.-Sezione di Roma, Italy; another (R.B.) was supported in part by I.N.F.N.-Sezione di Napoli, Italy.

APPENDIX

We present the spectrum of eigenvalues for the de Almeida–Thouless matrix G at first order of replica-symmetry breaking. These have been obtained following the process described in Ref. 14. If P_{ab} is the order-parameter matrix, let us suppose, at first order of replica-symmetry breaking, that $P_{ab}=p_1$ when the replicas a and b belong to the same subblock of size m and p_0 otherwise.

Then, we define the following averages:

$$\langle A\rangle=\int_{-\infty}^{\infty}\frac{dz}{(2\pi)^{1/2}}e^{-z^2/2}A\ , \tag{A1}$$

$$\overline{A}=\frac{\int_{-\infty}^{\infty}[dy/(2\pi)^{1/2}]e^{-y^2/2}\cosh^m[f(y,z)]A}{D(z)}\ , \tag{A2}$$

where $f(y,z)=\beta[p_0^{1/2}z+(p_1-p_0)^{1/2}y]$ and

$$D(z)=\int_{-\infty}^{\infty}\frac{dy}{(2\pi)^{1/2}}e^{-y^2/2}\cosh^m[f(y,z)]\ . \tag{A3}$$

If $k_1,k_2,\ldots$ define difference subblocks of the hierarchical matrix P_{ab}, we construct the following correlation functions:

$$p_1=\langle\sigma_a\sigma_b\rangle(a,b\in k)=\langle\overline{\tanh^2 f}\rangle\ ,$$

$$p_0=\langle\sigma_a\sigma_b\rangle(a\in k_1,b\in k_2)=\langle(\overline{\tanh f})^2\rangle\ ,$$

$$r_0=\langle\sigma_a\sigma_b\sigma_c\sigma_d\rangle(a,b,c,d\in k)=\langle\overline{\tanh^4 f}\rangle\ ,$$

$$r_1=\langle\sigma_a\sigma_b\sigma_c\sigma_d\rangle(a,b,c\in k_1,d\in k_2)=\langle\overline{\tanh^3 f}\,\overline{\tanh f}\rangle\ ,$$

$$r_2=\langle\sigma_a\sigma_b\sigma_c\sigma_d\rangle(a,b,\in k_1c,d\in k_2)=\langle(\overline{\tanh^2 f})^2\rangle\ ,$$

$$r_3=\langle\sigma_a\sigma_b\sigma_c\sigma_d\rangle(a,b\in k_1c\in k_2d\in k_3)$$
$$=\langle\overline{\tanh^2 f}(\overline{\tanh f})^2\rangle\ ,$$

$$r_4=\langle\sigma_a\sigma_b\sigma_c\sigma_d\rangle(a\in k_1b\in k_2c\in k_3d\in k_4)$$
$$=\langle(\overline{\tanh f})^4\rangle\ .$$

Then, we construct the different elements for the stability matrix G, which are

$$G_{(ab)(ab)}=P_1=1-\beta^2(1-p_1^2)/(ab)\in k\ ,$$

$$G_{(ab)(ab)}=P_0=1-\beta^2(1-p_0^2)/a\in k_1b\in k_2\ ,$$

$$G_{(ab)(ac)}=Q_0=\beta^2(p_0^2-p_1)/a\in k_1b,c\in k_2\ ,$$

$$G_{(ab)(ac)}=Q_1=\beta^2(p_1^2-p_1)/a,b,c\in k\ ,$$

$$G_{(ab)(ac)}=Q_2=\beta^2(p_0^2-p_0)/a\in k_1b\in k_2c\in k_3\ ,$$

$$G_{(ab)(ac)}=Q_3=\beta^2(p_0p_1-p_0)/a,b\in k_1c\in k_2\ ,$$

$$G_{(ab)(cd)}=R_0=\beta^2(p_1^2-r_0)/a,b,c,d\in k\ ,$$

$$G_{(ab)(cd)}=R_1=\beta^2(p_0p_1-r_1)/a,b,c\in k_1d\in k_2\ ,$$
$$\text{or } a\in k_1b,c,d\in k_2\ ,$$

$$G_{(ab)(cd)}=R_2=\beta^2(p_1^2-r_2)/a,b,\in k_1c,d\in k_2\ ,$$

$$G_{(ab)(cd)}=R_3=\beta^2(p_0^2-r_2)/a,c\in k_1b,d\in k_2\ ,$$

$$G_{(ab)(cd)}=R_4=\beta^2(p_0p_1-r_3)/a,b\in k_1c\in k_2d\in k_3\ ,$$
$$\text{or } a\in k_1b\in k_2c,d\in k_3\ ,$$

$$G_{(ab)(cd)}=R_5=\beta^2(p_0^2-r_3)/a\in k_1b,c\in k_2d\in k_3\ ,$$

$$G_{(ab)(cd)}=R_6=\beta^2(p_0^2-r_4)/a\in k_1b\in k_2c\in k_3d\in k_4\ .$$

The spectrum of eigenvectors contains three invariant sectors. We present the eigenvalues and degeneracies for finite n. Finally, the analytic continuation $n\to 0$ has to be performed.

1. Longitudinal invariant sector

It contains two eigenvalues each one with degeneracy equal to 1. These are obtained by solving a second degree equation:

$$\lambda_L=\frac{A+D\pm\sqrt{(A-D)^2+4BC}}{2}\ ,$$

$$A=P_1+2(m-2)Q_1+\frac{(m-3)(m-2)}{2}R_0$$
$$+\frac{(n-m)(m-1)}{2}R_2\ ,$$

$$B=2(n-m)Q_3+(n-m)(m-2)R_1$$
$$+\frac{(n-m)(n-2m)}{2}R_4\ , \tag{A4}$$

$$C=2(m-1)Q_3+(m-2)(m-1)R_1$$
$$+\frac{(n-2m)(m-1)}{2}R_4\ ,$$

$$D=P_0+2(m-1)Q_0+2(n-2m)Q_2+(m-1)^2R_3 +2(m-1)(n-2m)R_5+\frac{(n-3m)(n-2m)}{2}R_6 .$$

2. Anomalous invariant sector

We have four eigenvalues. Two of them coincide with the longitudinal ones in the limit $n\to 0$ and have degeneracy equal to $(n-m)/m$. The other two eigenvalues have a degeneracy equal to $n(m-1)/m$ and are also given by a second degree equation:

$$\lambda_A=\frac{A+D\pm\sqrt{(A-D)^2+4BC}}{2} , \tag{A5}$$

$$A=P_1+(m-4)Q_1-(m-3)R_0 ,$$

$$B=\frac{(n-m)(m-2)}{(m-1)}(Q_3-R_1) ,$$

$$C=(m-1)(Q_3-R_1) ,$$

$$D=P_0+(m-2)Q_0+(n-2m)Q_2 -(m-1)R_3-(n-2m)R_5 .$$

3. Third invariant sector

We have four eigenvalues:

$$\lambda_R^1=P_1-2Q_1+R_0 \quad \left[d=\frac{n(m-3)}{2} \right] ,$$

$$\lambda_R^2=P_0+2(m-1)Q_0-2mQ_2+(m-1)^2R_3 -2m(m-1)R_5+m^2R_6 \quad \left[d=\frac{(n-3m)n}{2m^2} \right] ,$$

$$\lambda_R^3=P_0+(m-2)Q_0-mQ_2-(m-1)R_3+mR_5 \quad \left[d=\frac{n(n-2m)(m-1)}{m^2} \right] ,$$

$$\lambda_R^4=P_0-2Q_0+R_3 \quad \left[d=\frac{n(m-1)^2(n-m)}{2m^2} \right] .$$

These results have been given in the literature near T_c. The spectrum we give is valid at all temperatures.

[1] S. Cabasino, E. Marinari, P. Paolucci, and G. Parisi, J. Phys. A. **21**, 4201 (1988).
[2] W. A. Little, Math. Biosci. **19**, 101 (1974).
[3] D. Sherrington and S. Kirkpatrick, Phys. Rev. Lett. **35**, 1792 (1975); Phys. Rev. B **17**, 4384 (1978).
[4] D. J. Amit, H. Gutfreund, and H. Sompolinsky, Phys. Rev. A **32**, 1007 (1985).
[5] A. P. Young and S. Kirkpatrick, Phys. Rev. B **25**, 440 (1982).
[6] K. Binder and A. P. Young, Rev. Mod. Phys. **58**, 801 (1986).
[7] M. Mézard, G. Parisi, and M. A. Virasoro, *Spin Glass Theory and Beyond,* Lectures Notes in Physics Vol. 9 (World Scientific, Singapore, 1987).
[8] C. de Dominicis and A. P. Young, J. Phys. A **16**, 2063 (1983).
[9] A. J. Bray and M. A. Moore, J. Phys. C **13**, 419 (1980).
[10] J. R. de Almeida and D. J. Thouless, J. Phys. A **11**, 983 (1978).
[11] G. Parisi, Phys. Lett. **73A**, 203 (1979).
[12] G. Parisi, J. Phys. A **13**, 1101 (1980).
[13] C. De Dominicis and I. Kondor, Phys. Rev. B **27**, 606 (1983).
[14] C. De Dominicis and I. Kondor, in *Applications of Field Theory to Statistical Mechanics,* Lecture Notes in Physics Vol. 216, edited by L. Garrido (Springer-Verlag, Berlin, 1985).
[15] R. G. Palmer and C. M. Pond, J. Phys. F **9**, 1451 (1979).